

PUBLISHED VERSION

Mahmoud, Saleh; Medwell, Paul Ross; Dally, Bassam; Alwahabi, Zeyad T.; Nathan, Graham [Simultaneous measurements of temperature and soot volume fraction in turbulent diffusion flames](#) Proceedings of the Australian Combustion Symposium, Perth, WA, 6-8 November 2013 / Mingming Zhu, Yu Ma, Yun Yu, Hari Vuthaluru, Zhezi Zhang and Dongke Zhang (eds.): pp.104-107

The copyright of the individual papers contained in this volume is retained and owned by the authors of the papers.

PERMISSIONS

<http://www.anz-combustioninstitute.org/local/papers/ACS2013-Conference-Proceedings.pdf>

Reproduction of the papers within this volume, such as by photocopying or storing in electronic form, is permitted, provided that each paper is properly referenced.

The copyright of the individual papers contained in this volume is retained and owned by the authors of the papers. Neither The Combustion Institute Australia & New Zealand Section nor the Editors possess the copyright of the individual papers.

Clarification of the above was received 12 May 2014 via email, from the Combustion Institute anz

12 May 2014

<http://hdl.handle.net/2440/82564>

Simultaneous Measurements of Temperature and Soot Volume Fraction in Turbulent Diffusion Flames

*S. Mahmoud^{a,b}, P. R. Medwell^{a,b}, B. B. Dally^{a,b}, Z. T. Alwahabi^{a,c}, and G. J. Nathan^{a,b}

^aCentre for Energy Technology, ^bSchools of Mechanical and ^cChemical Engineering
The University of Adelaide, S.A. 5005, AUSTRALIA

Abstract

Spatially resolved two-dimensional temperature and soot volume fractions were measured simultaneously in a turbulent non-premixed attached jet flame, using non-linear two-line atomic fluorescence (NTLAF) and laser induced incandescence (LII) techniques, respectively. Measurements were performed in a well characterised Ethylene-Hydrogen-Nitrogen jet flame in such a way as to avoid any significant interference of the two laser diagnostic techniques on each other. Laser ablation was used to seed Indium atoms into the flame for the temperature measurements. Sample images of single-shot simultaneous temperature and soot concentration images are presented at one location. Joint probability density functions (pdf's) of soot volume fraction (SVF) as a function of temperature are also reported. The strong influence of temperature on SVF is found to be consistent with the current understanding and highlights the importance of the simultaneous measurements for understanding soot behaviour in a turbulent environment and for providing reliable data for soot model validation.

Keywords: Temperature, Soot, Ablation, Simultaneous, Two-line atomic fluorescence, Laser-induced incandescence.

1. Introduction

Soot is a common and important species in most combustion systems. The processes of soot formation and destruction in practical environments are highly complex, as they are associated with interdependent parameters such as fuel type, temperature, pressure, soot concentration, strain rate, and mixture fraction [1]. Many of these parameters are coupled in the case of turbulent flows. Of these dependencies, the relationship between soot concentration and temperature is of primary importance to the understanding of soot, but is yet to be reported in a turbulent environment [2].

Soot and temperature have an intrinsic coupled dependence since temperature is one of the parameters that govern the formation and destruction processes of soot in a flame. Soot concentration and distribution, at the same time, influences temperature due to the heat transfer through incandescent radiation from soot particles [3,4]. For this reason, a thorough understanding of soot evolution in a flame depends on the knowledge of temperature. While simultaneous measurements of different parameters are required to characterize and describe a flame [5], it is also highly desirable that the measurements involve more than one dimension in a turbulent environment, allowing the acquisition of spatially correlated scalars and their gradient, which are of a great benefit in understanding of soot evolution and in the study of practical combustion systems [5,6].

The concurrent application of two non-intrusive planar techniques offer the advantage of two dimensional

imaging which is essential for characterizing the behaviour of soot sheets and its interaction with the local temperature fields. Chan et al. [4] demonstrated the applicability of joint NTLAF-LII measurements to assess the coupled dependencies of temperature and soot, however, their measurements were performed in laminar and wrinkled flames only. Simultaneous planar measurements of temperature and soot concentration in a turbulent diffusion jet flame have not been reported previously.

It is well known that major advances in combustion research come from the joint application of reliable experimental data and detailed CFD model development, therefore there is a need for the experiments to be performed under conditions which are very well characterized. However, while most available experimental databases offer well characterized turbulent flame conditions, there is no current experimental platform that offers simultaneous measurements of temperature and soot concentration in a well characterized and attached turbulent jet flame. [5,7,8]. Hence there is a need for this data.

For these reasons, the first aim of the present investigation is to demonstrate the simultaneous and planar, single-shot imaging of temperature and soot volume fraction in a turbulent environment, for the first time. The second aim is to provide new insight into the evolution of soot in a well characterised, attached turbulent flame from a statistical assessment of these data, while also supporting model development and validation.

* Saleh Mahmoud:
Phone: (+61) 4 16647253
Email: saleh.mahmoud@adelaide.edu.au

2. Experimental Setup

2.1. Burner details

The burner used in this experiment consists of a circular aluminium tube of 4.4 mm ID with a tapered end at the jet outlet and a wall thickness of 1mm. The burner is mounted in the centre of a contraction delivering co-flowing air at ambient temperature and at a bulk velocity of 0.7m/sec. The contraction has a square cross-section of dimensions 150mm by 150mm, and the pipe jet burner outlet rises above the contraction edge by a distance of 18mm.

The fuel composition of the flame is 40% ethylene, 40% hydrogen, and 20% nitrogen (by volume). The total mixture density at 294K and 100 KPa is calculated to be 0.727 Kg/m³, while the total viscosity (dynamic) is calculated to be 1.212×10⁻⁵ kg/m.s. More details of the flow conditions are provided in **Table 1**.

The mean velocity and the turbulence intensity of the flow from the nozzle and the co-flow at the nozzle exit plane are presented in **Fig.1**. Good symmetry was found. Therefore, temperature and soot volume fraction measurements were performed only on the left (laser-in) side of the flame.

A traverse was used to move the burner vertically through the optical diagnostic beams to enable measurements through the entire flame. The flame length, as determined from the time-averaged photographs of the flame in **Fig.2**, was measured to be 170 nozzle diameters (~750mm) from the fuel nozzle under the specified experimental conditions. Although measurements were performed at ten different locations spanning various regions across the flame height, data here are only reported at 120 nozzle diameters (450mm) downstream from the exit plane.

Table1. Initial flow conditions for the attached jet flame.

Attached Jet Flame	Composition		Total Flow rate	Average Velocity	Exit Strain Rate	Reynolds number	
	Mass Flow Rate	Vol. Flow Rate					
	(g/s)	(l/min)					
Mixture	C ₂ H ₄	0.40213	20.8	52.0	57.0	12.95	15,000
	H ₂	0.2867	20.8				
	N ₂	0.19933	10.4				

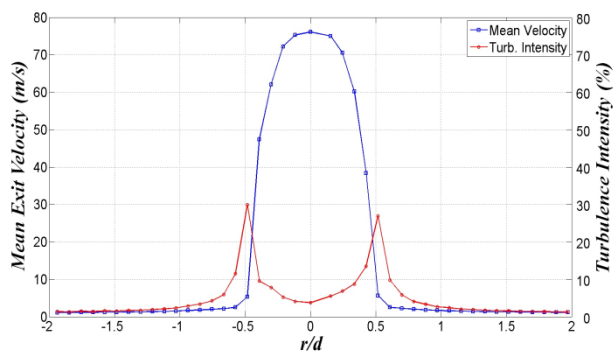


Fig.1. Velocity Profile (in blue) and turbulence Intensity profile (in red) from both the jet and the co-flow at a height of 1mm above the exit plane of the nozzle. Jet diameter d is 4.4 mm.

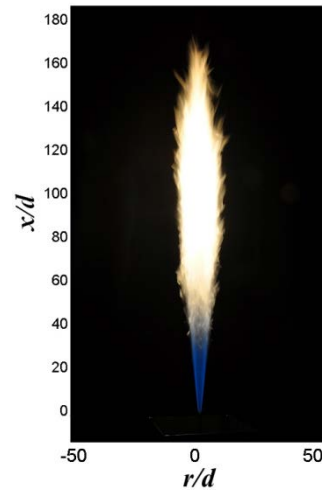


Fig.2. Real color photograph of the investigated attached jet flame, burning a mixture of ethylene, hydrogen, and nitrogen.

2.2 Indium Ablation

Indium ablation was selected to seed the jet flame as it can successfully deliver indium far downstream in a turbulent flow, while achieving a high signal to noise ratio [9]. It also allows the probing of the low temperature regions of the flame, which is not possible with the nebuliser seeding of indium chloride with a solvent. Furthermore, seeding by “ablation” avoids the addition of large concentration of solvents into the flame, and tends to preserve the flame original volumetric composition. [6,9].

The laser ablation technique follows the same arrangement that has been described in previous publications [6, 9]. In brief, the laser ablation method uses a pulsed and focused high energy laser beam to remove metal from a surface by rapid heating, thus releasing indium atoms. The system involves a 10 mm diameter indium rod mounted on a motorized rotating shaft and placed within an ‘ablation chamber’. The rod is exposed to a 10 Hz focused, second harmonic output laser beam (532 nm) of a Q-switched Nd:YAG laser. The resulting ablation products are transported by the fuel stream from the chamber into the jet burner.

2.3. NTLAF experimental setup

The experimental arrangement for NTLAF is shown in **Fig. 3**. Two Nd:YAG pumped dye lasers are tuned to 410.18 and 451.13 nm and fired with 100 ns separation. The two beams are combined into a co-planar sheet of 0.3 mm thickness and 20 mm height. Profile variation across the sheet height was also recorded by a third Megaplex camera allowing shot-by-shot correction of the laser energy. Fluorescence from the flame was detected through two intensified CCD (ICCD) cameras using f#1.4 lenses.

2.4. LII experimental setup

Soot volume fraction was measured using the LII technique. Excitation was performed with an Nd:YAG laser at 1064 nm, while the incandescence was collected

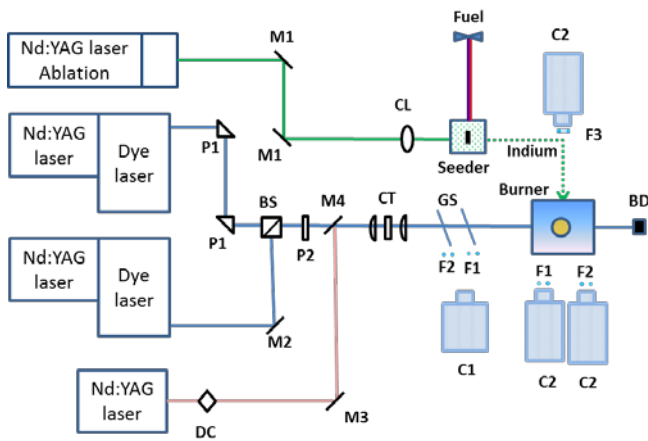


Fig.3: Schematic diagram of the optical arrangement. BS, beam splitter; BD, beam dump; C, camera; CL, cylindrical lens; CT, cylindrical telescope; DC, doubling crystal; F, optical filter; GS, glass slide; M, mirror; P1, prism; P2, circular polarizer.

with another ICCD camera with a 430-nm (10 nm bandwidth) interference filter. This arrangement was selected to minimise interferences [7]. To avoid any crosstalk between the LII and the NTLAF imaging, a time delay of 800 ns was applied between the NTLAF and the LII measurements. This delay, being small compared to the physical and chemical time-scales of the flame, ensures that the NTLAF and LII measurements are effectively simultaneous. The gate-width of the LII was set to 50 ns, while the timing was set to coincide with the LII excitation, as this is proven to decrease the sensitivity of the signal to the soot particle sizes [10]. The LII laser sheet was approximately 30 mm high and 0.3 mm thick. The LII signal is expected to be independent of the fluence variation, since the operating laser fluence of the LII beam was kept at 1 J/cm^2 (above the plateau region of the LII response curve) throughout the experiment.

Calibration of the LII signal was performed on a Mckenna-type burner using laser extinction, where a continuous-wave 1064 nm laser was used instead of a 632-nm beam to avoid absorption effects (from PAH, or other particles) [7].

2.5. Image Processing

The resultant images from all three cameras (Stokes, anti-Stokes, and LII) are spatially matched using a seven-point matching algorithm and morphed based on the cross-correlation of a transparent target to ensure sub-pixel matching of the images. Temperature images are deduced from the ratio of the Stokes to the anti-Stokes signals, while the soot volume fraction images are obtained from the LII images. Temperatures below 800K are set to zero as Indium cannot be detected below that temperature, while the soot detection limit is set at 80 ppb. Simultaneous single shot images of temperature and soot concentration are presented in the next section.

3. Results and Discussion

Figures 4 and 5 present two typical simultaneous image pairs (single shot) of temperature, soot volume fraction, 450mm downstream from the jet exit.

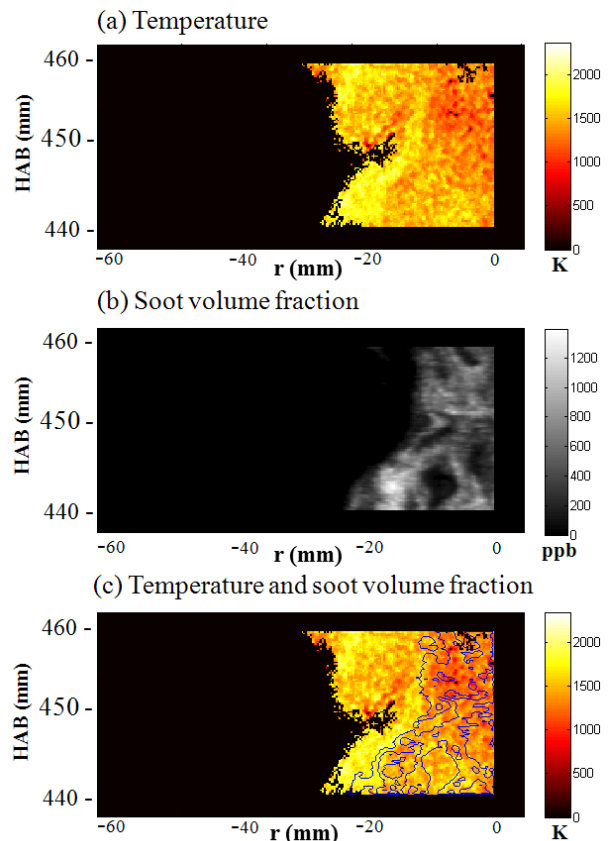


Fig.4. Selected simultaneous single-shot images of the left side of an axis-symmetric turbulent non premixed ethylene, hydrogen, and nitrogen flame. (a) NTLAF temperature, (b) LII soot volume fraction, and (c) instantaneous temperature field with contours of soot overlaid (in blue). Laser propagation from left to right.

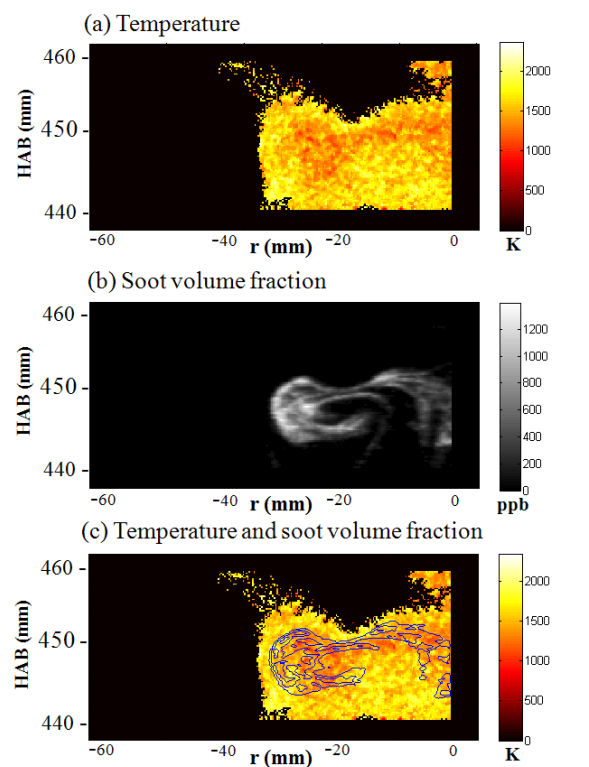


Fig.5. Selected simultaneous single-shot images (a) NTLAF temperature, (b) LII soot volume fraction, and (c) instantaneous temperature field with contours of soot overlaid (in blue).

It is observed that the presence of soot sheets, although being intermittent, is directly related to the local temperature zone. An “inverse” correlation between soot and temperature is deduced from these images, where soot tends to increase in concentration around low temperature fields, while rarely overlapping the high temperature zone. It is noticed that the soot sheets are typically bordering the stoichiometric region of the flame and are confined to the fuel rich side of the flame, with no record of soot escaping to the air side of the flame. While this correlation does not exactly hold for locations further upstream the 450mm location (not reported here), the soot concentration is observed to be inherently linked to the flame temperature at various other heights throughout the flame. This outcome is consistent with previous simultaneous measurements of soot and temperature performed in a wrinkled flame [4].

The correlation between soot concentration and temperature at the selected height is further examined from Fig.6, which presents PDF's of instantaneous volume fraction binned into 200 K temperature bands for the same flame height of the instantaneous images (450 mm). It can be seen that a much wider range of soot volume fraction values is associated with lower temperatures than for high temperature bands, which exhibit a narrower range. A soot range of 0.08 ppm (minimum detection limit) to 1 ppm exists at an equal probability within the lowest detectable temperature band (800 to 1000K), while lower soot volume fractions are more probable in the temperature bands. It is also deduced that, although soot is more probable at high temperatures, it is found there at relatively low concentrations. The probability decreases with the temperature, but spans a broader range of soot volume fraction values. Further analysis of these data at this height and at various other locations is underway and will be released in future publications.

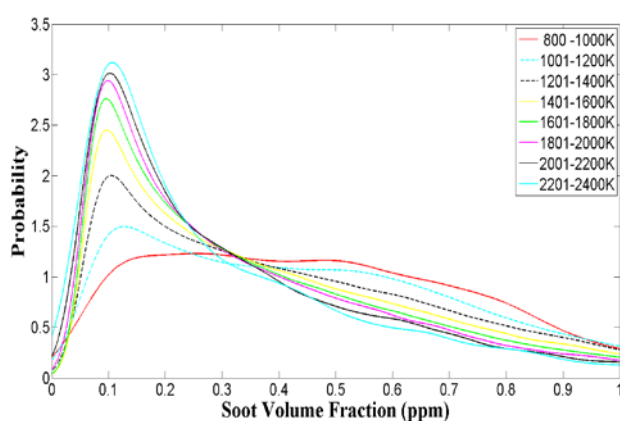


Fig.6: PDF's of instantaneous volume fraction binned into bands of 200 K temperature across the flame at a height of 450mm downstream.

4. Conclusion

The first instantaneous and simultaneous planar imaging of temperature and soot concentration in a turbulent and attached diffusion jet flame has been demonstrated using nonlinear regime two-line atomic fluorescence (NTLAF) and laser-induced incandescence (LII) techniques, respectively. The images presented at one location reveal a strong correlation between instantaneous soot volume fraction and the local temperature field, and demonstrate the applicability of joint NTLAF–LII measurements to assess the coupled dependency of temperature and soot in flames. The joint pdf's of soot concentration as a function of temperature bands reveals that the soot volume fraction at this location is a strong function of temperature. A broader range of soot concentration is found at the lower temperatures, while the range of concentration is narrower at higher temperature. This study represents a significant breakthrough in the diagnostic capabilities in sooty turbulent flames, which is crucial for the detailed understanding of the coupled dependence of temperature and soot in flames of practical significance.

5. Acknowledgments

The authors acknowledge the support of the Centre for Energy Technology and The University of Adelaide. The Australian Research Council is also gratefully acknowledged for their funding support of this work through ARC Discovery grant.

6. References

- [1] J.H. Kent, D. Honnery, *Combust. Sci. Technol.* **54** (1987) 383–397.
- [2] K.P. Geigle, Y. Schneider-Ku'hnle, M.S. Tsurikov, R. Hedef, R. Lu'ckerath, V. Kru'ger, W. Stricker, M. Aigner, *Proc. Combust. Inst.* **30** (2005) 1645–1653.
- [3] B.S. Haynes, H.G. Wagner, *Prog. Energy Combust.Sci.* **7** (1981) 229–273.
- [4] Q. N. Chan, P. R. Medwell, P. A. M. Kalt, Z. T. Alwahabi, B. B. Dally, G. J. Nathan, *Proc. Combust. Inst.* **33** (2011) 791–798.
- [5] R.S. Barlow, *Proc. Combust. Inst.* **31** (2007) 49–75.
- [6] P.R. Medwell, Q.N.Chan, B.B. Dally, S. Mahmoud, Z.T. Alwahabi, G.J. Nathan, *Proc. Combust. Inst.* **34** (2013) 3619–3627.
- [7] N.H. Qamar, Z.T. Alwahabi, Q.N. Chan, G.J.Nathan, D. Roekaerts, K.D. King, *Combustion and Flame* **156**(7) (2000) 1339-1347.
- [8] W. Meier, R. S. Barlow, Y.-L. Chen, J.-Y. Chen, *Combustion and Flame* **123** (2000) 326–343.
- [9] P. R. Medwell, Q. N. Chan, B. B. Dally, Z. T. Alwahabi, S. Mahmoud, G. F. Metha, G. J. Nathan, *Applied Physics B: Applied Physics B* **107**(3) (2012) 665-668.
- [10] R.L. Vander Wal, *Appl. Opt.* **35** (1996) 6548–6559.